Optica Applicata, Vol. XXXIX, No. 2, 2009

Multi-stage ring resonator all-pass filters for dispersion compensation

CHINDA CHAICHUAY[1], PREECHA P. YUPAPIN[2*], PRAJAK SAEUNG[3*]

[1]Department of Mathematics and Computer Science, Faculty of Science,
King Mongkut's Institute of Technology Ladkrabang, Bangkok 10520, Thailand

[2]Advanced Research Center for Photonics, Department of Applied Physics, Faculty of Science,
King Mongkut's Institute of Technology Ladkrabang, Bangkok 10520, Thailand

[3]Electronics Technology Division, Department of Physics, Faculty of Science,
Ramchamhaeng University, Bangkok 10240, Thailand

[*]Corresponding authors: P. Saeung – prajak_neer27@hotmail.com; P.P. Yupapin – kypreech@kmitl.ac.th

This paper describes group delay time property of the multi-stage ring resonator all-pass filters (RRAPF) in either cascading single stages or using lattice architectures. The present analysis is restricted to directional couplers and waveguides characterized by various parameters, and careful design of these parameters can optimize the group delay response. The extra phase shifters of each single stage have been adjusted to yield a broadband group delay. By increasing the number of filter stages, a larger bandwidth over the dispersion can be obtained. This device is able to provide dispersion compensation to systems such as the high speed dense wavelength division multiplexer (DWDM) for the optical fiber communication system.

Keywords: ring resonator, all-pass filter, group delay, quadratic dispersion.

1. Introduction

The basic type of an autoregressive moving average (ARMA) planar waveguide filter is a single ring resonator connected to one coupler which provides no path back to the input port. This filter is called an all-pass or, in the absence of loss, unit transmittance networks [1], because the magnitude of their transmission factor is unity on the whole spectrum, independent of wavelength. Although lossless all-pass filters do not display magnitude filter characteristics, their phase response is frequency dependent. Therefore, they can be configured for group delay equalization and dispersion compensation [2–4], polarization mode dispersion compensation [5], and other applications based on their phase-frequency characteristics such as band-pass filtering when used in conjunction with other optical components. There have been growing interests in tunable dispersion compensators (TDC) for high-speed wavelength division multiplexed (WDM) networks. This is because the chromatic dispersion of transmission path could be changed frequently in a dynamically reconfigurable WDM networks. The TDC based on a ring resonator all-pass filter is one of the key components in these networks. Optical ring resonator all-pass filters (RRAPF) can be realized using multi-stage ring resonator in either cascading single stages or using lattice architectures [6]. In this paper, multi-stage RRAPF for dispersion compensation is proposed and analyzed. Desired group delay shape, which has a larger value and is sharper, can be tuned by the amount of power coupling to the ring.

2. Transfer functions of ring resonator all-pass filters

2.1. Cascaded ring resonator all-pass filters

The architecture of single ring and three stage cascaded RRAPF is illustrated in Fig. 1, whose every stage is constructed by one ring resonator and one 2×2 optical coupler. The insertion loss of the coupler γ and κ_i is the coupling factor of the i-th coupler. When a coherent source is input into a device, the coupling intensity for the throughput path in each stage is denoted by $c_i = \sqrt{1 - \kappa_i}$ and for the cross path it is $-js_i = -j\sqrt{\kappa_i}$, where $-j$ represents the $-(\pi/2)$ phase shift. As to the transmission of light along the ring resonator (the closed pass), we can represent as xz^{-1}, where $x = \exp(-\alpha L/2)$ is the one round-trip losses coefficient, and the z^{-1} is the Z-transform parameter, which is defined in terms of normalized angular frequency ω as

$$z^{-1} = \exp(-j\omega) = \exp(-j\beta L) \tag{1}$$

where $\beta = kn_{\text{eff}}$ is the propagation constant, $k = 2\pi/\lambda$ is the vacuum wave number, n_{eff} is the effective refractive index of the waveguide and the circumference of the ring is $L = 2\pi R$, here R is the radius of the ring.

When all rings have the same circumference, a device we call a uniform cascaded RRAPF. Therefore, each single stage has the same periodic resonant responses in the frequency domain with the free spectral range (FSR) between two resonance peaks given by

$$\text{FSR} = \Delta f = \frac{c}{n_g L} \tag{2}$$

where $n_g = n_{\text{eff}} + f_o(\mathrm{d}n_{\text{eff}}/\mathrm{d}f)_{f_o}$ is the group index of the ring waveguide, f_o is the center frequency and c is the velocity of light in vacuum. The optical resonators resonate at a high order mode. At the f_o, the perimeter of the ring is an integer number of guide wavelengths, and this integer M_r is the order number of mode and $f_o = M_r\text{FSR}$. Using the scattering matrix with Z-transform or signal flow graph technique as in [7, 8], we can express the transfer function for single RRAPF by

$$S(z) = \frac{E_o}{E_i} = \frac{c - xz^{-1}}{1 - cxz^{-1}} \tag{3}$$

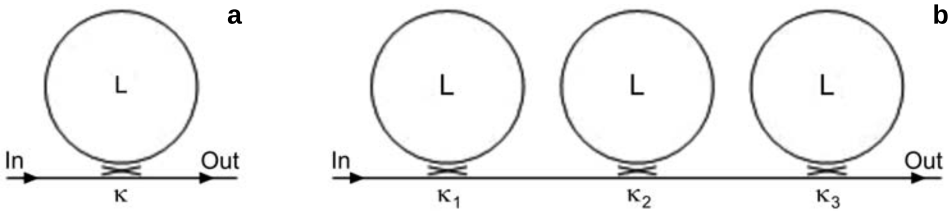

Fig. 1. Schematic layout of single ring (**a**), and three stage cascaded RRAPF (**b**).

By evaluating $S(z)$ at $z = \exp(j\omega)$ and defining the phase delay by $S(\omega) = |S(\omega)|\exp(j\theta(\omega))$, we obtain from (3) the relative intensity transfer

$$|S|^2 = \frac{c^2 + x^2 - 2xc\cos(\omega)}{1 + (cx)^2 - 2xc\cos(\omega)} \tag{4}$$

and the phase delay is given by

$$\theta(\omega) = \tan^{-1}\left[\frac{x(1-c^2)\sin(\omega)}{c(1+x^2) - x(1+c^2)\cos(\omega)}\right] \tag{5}$$

The resonances for Fig. 1**a** occur at frequencies where $\cos(\omega) = 1$, that are at $f = M_r c/n_{\text{eff}} L$. The minimum transmission of $|S|^2$ at resonance is

$$|S|^2_{f_o} = \frac{(c-x)^2}{(cx-1)^2} \tag{6}$$

and if the coupling coefficient reaches the critical value of $\kappa = \kappa_c = 1 - x^2$, the intensity reaches zero, and there is no transmission, *i.e.*, the fractional loss around the ring is exactly the same as the fractional loss through the coupler.

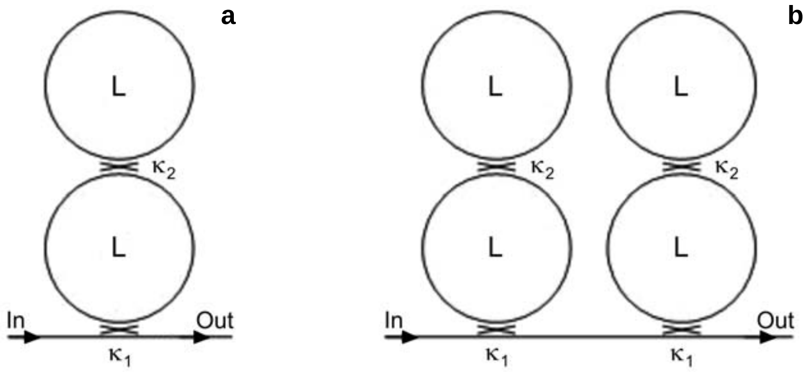

Fig. 2. Schematic layout of two stage lattice RRAPF (**a**), and lattice RRAPF 2×2 array (**b**).

2.2. Lattice ring resonator all-pass filters

Figure 2 illustrates the two stage lattice RRAPF and lattice RRAPF 2×2 arrays which the improved group delay can be obtained. For simplicity, the waveguide is considered lossless so that $x = 1$, the transfer function of Fig. 2**a** can be expressed as

$$S = \frac{E_o}{E_i} = \frac{c_1 - \exp\left[-j(\omega - \phi)\right]}{1 - c_1 \exp\left[-j(\omega - \phi)\right]} \tag{7}$$

where ϕ is the phase delay shift resulting from the upper ring resonator which is given by

$$\phi(\omega) = \tan^{-1}\left[\frac{(1 - c_2^2)\sin(\omega)}{2c_2 - (1 + c_2^2)\cos(\omega)}\right] \tag{8}$$

3. Group delay of ring resonator all-pass filters

The filter's group delay is defined as the negative derivative of the phase of the transfer function with respect to the angular frequency as follows [6]:

$$\tau_n(\omega) = -\frac{\mathrm{d}\theta(\omega)}{\mathrm{d}\omega} = -\frac{\mathrm{d}}{\mathrm{d}\omega}\tan^{-1}\left\{\frac{\mathrm{Im}[S(z)]}{\mathrm{Re}[S(z)]}\right\}_{z = \exp(j\omega)} \tag{9}$$

where τ_n is normalized to the unit delay of the waveguide T. The absolute group delay is given by $\tau_g = T\tau_n$. Thus, we substitute (5) into (9) and given that $\mathrm{d}\tan^{-1}[g(x)]/\mathrm{d}x = g'(x)/[1 + g^2(x)]$, the normalized group delay of Fig. 1**a** is given explicitly in terms of c, x and ω as follows:

$$\tau_n(\omega) = \frac{x(1 - c^2)\left[x(1 + c^2) - (1 + x^2)c\cos(\omega)\right]}{\left[x(1 + c^2) - (1 + x^2)c\cos(\omega)\right]^2 + \left[(1 - x^2)c\sin(\omega)\right]^2} \tag{10}$$

Equation (10) is a periodic group delay response in frequency domain, which exhibits sharp peaks at $\omega = 2M_r\pi$. The value of (10) at resonance where $\cos(\omega) = 1$ is

$$\tau_n\big|_{f_o} = \frac{x(1 - c^2)}{x(1 + c^2) - (1 + x^2)c} \tag{11}$$

The normalized group delay as a function of normalized angular frequency ω for a lossless waveguide is given by

$$\tau_n\big|_{x = 1} = \frac{1 - c^2}{1 + c^2 - 2c\cos(\omega)} \tag{12}$$

which simplifies to

$$\tau_n\Big|_{f_o,\,x\,=\,1} = \frac{1+c}{1-c} \tag{13}$$

In the case of the three stage cascaded RRAPF as in Fig. 1**b**, it can be shown that the normalized group delay τ_n which is the sum of the individual normalized group delay τ_{ni} is induced by each single stage ring resonator. For a lossless waveguide τ_n is given by

$$\tau_n(\omega) = \sum_{i=1}^{3} \tau_{ni}(\omega) = \sum_{i=1}^{3} \frac{1-c_i^2}{1+c_i^2-2c_i\cos(\omega)} \tag{14}$$

The extra tunable phase shifters of each single stage can be added to yield a broadband group delay. Therefore, in this case, the result in (14) in term of $\cos(\omega)$ which is replaced by $\cos(\omega+\varphi_i)$, where φ_i is an additional phase shift of each ring.

Similarly, by using Eqs. (7) and (8), we obtain from (9) the normalized group delay τ_n of the lattice RRAPF 2×2 array (as Fig. 2**b**) is expressed by

$$\tau_n(\omega) = \sum_{i=1}^{2} \tau_{ni}(\omega) =$$

$$= \sum_{i=1}^{2} \left[\frac{1-c_{1i}^2}{1+c_{1i}^2-2c_{1i}\cos(\omega-\phi_i)} \left(1+\frac{1-c_{2i}^2}{1+c_{2i}^2-2c_{2i}\cos(\omega)} \right) \right] \tag{15}$$

where c_{1i}, c_{2i} are the coupling intensity coefficients for the throughput path of the *i*-th column for lattice RRAPF 2×2 array. The resonance of Fig. 2**a** occurs at frequency where $\omega = 2\pi$ and $\phi = \pi$, due to the fact that the light from the upper ring must pass through the coupled arm of the upper coupler twice. The value of (15) at resonance for Fig. 2**a** is then given by

$$\tau_n\Big|_{f_o} = \frac{2(1-c_1)}{(1+c_1)(1-c_2)} \tag{16}$$

Using identical symmetrical couplers $\kappa_1 = \kappa_2$, the normalized group delay in (16) at resonance simplifies to small value of $2/(1+c_1)$.

4. Simulation results

The normalized group delay response of single RRAPF in Fig. 1**a** is shown in Fig. 3. The parameters of the circuit used for this simulation were the design frequency (wavelength) $f_o = 193.1$ THz ($\lambda_o = c/f_o = 1552.52$ nm), $M_r = 1931$, FSR = 100 GHz and $n_g = 3.46$ (for the III–V semiconductor materials waveguide), which determines the circumference of the ring as $L = M_r \lambda_o / n_g$ =0.86 mm. The internal ring losses are assumed to be fully compensated ($\alpha = 0$). The normalized group delay response is periodic functions of the frequency of 100 GHz, which is the same as the FSR of the ring resonator and it has been found that as κ is decreased it became sharper and steeper at the resonant point.

Figure 4 is a plot of the normalized group delay of Fig. 1**a** by varying six values of round trip losses coefficient x based on Eq. (10). The coupling coefficient is fixed to be $\kappa = 0.2$ and the other parameters are the same as those used for Fig. 3. The critical value of the round trip losses coefficient is calculated to be $x_c = (1 - \kappa)^{1/2} = 0.894$. For $x > x_c$ the normalized group delay has a positive peak at resonance indicating that the signal is trapped and spends a relatively long time circulating in the ring. After

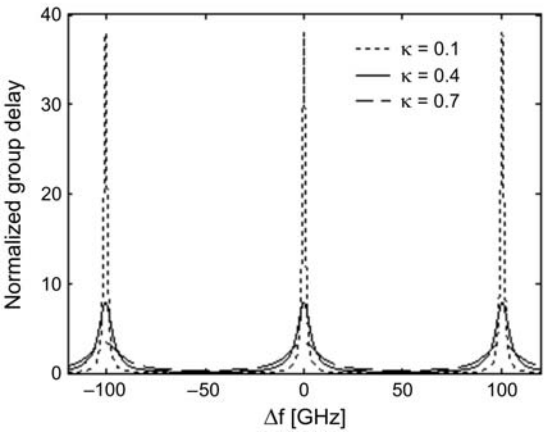

Fig. 3. Normalized group delay response of single RRAPF with lossless as in Fig. 1**a** comparing different coupling coefficients of $\kappa = 0.1$, 0.4 and 0.7.

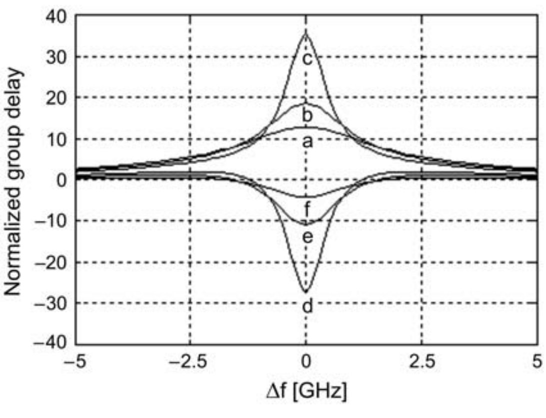

Fig. 4. Normalized group delay response of single RRAPF as in Fig. 1**a** by keeping κ fixed and varying round trip losses coefficient as: $x = 0.978$ (*a*), $x = 0.947$ (*b*), $x = 0.926$ (*c*), $x = 0.872$ (*d*), $x = 0.860$ (*e*), and $x = 0.834$ (*f*).

decreasing x, while keeping κ fixed, τ_n becomes sharper and large positive as x approaches its critical value, then flips to a large negative value and sharper as x is in the region $x < x_c$ and finally decreases in magnitude (remaining negative and broader) as x is further decreased. As we see, the result in Fig. 4 is following: the parameter is x when κ is fixed. Similarly, the same group delay response is realized for a fixed x under a variable κ as shown in Fig. 5. Here, the round trip losses coefficient is set to be $x = 0.894$, which results in critical value of $\kappa_c = (1 - a)^{1/2} = 0.2$.

A difficulty with the single-stage RRAPF is that the group delay response and the bandwidth over which a desired response can be approximated are limited. By using multi-stage RRAPF, a desired response can be more closely approximated, and it can be achieved over a broader portion of the period compared to single-stage RRAPF. Figure 6 shows the group delay response using three stage cascaded RRAPF as in Fig. 1**b** for compensation filter dispersion. The parameters of each ring resonator

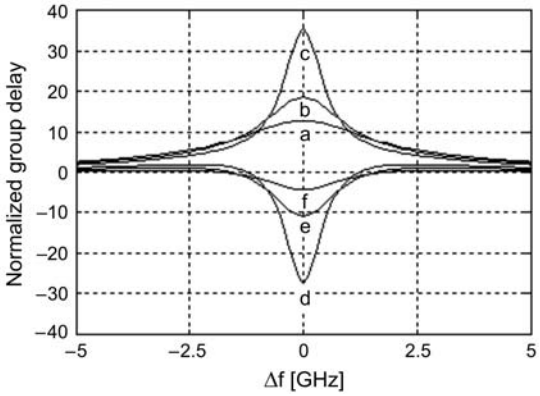

Fig. 5. Normalized group delay response of single RRAPF as in Fig. 1**a** by keeping x fixed and varying coupling coefficient as: $\kappa = 0.35$ (a), $\kappa = 0.30$ (b), $\kappa = 0.25$ (c), $\kappa = 0.15$ (d), $\kappa = 0.10$ (e), and $\kappa = 0.05$ (f).

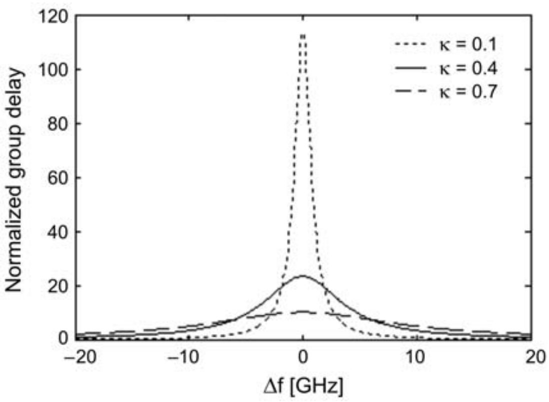

Fig. 6. Normalized group delay response of three stage cascaded RRAPF with lossless as in Fig. 1**b** for various identical coupling coefficients in each stage of $\kappa = 0.1$, 0.4, and 0.7.

are identical and the circumference of each ring is 0.86 mm. As a result (shown in Fig. 6), a larger bandwidth or FWHM over which the dispersion can be obtained due to increasing the number of filter stages.

By appropriately adjusting the coupling coefficient κ_i and the phase shift φ_i of each single stage, a broadband group delay response can be achieved as shown in Fig. 7. The delay curve of a ring resonator always has a constant surface independent of the coupling coefficient κ_i. As a consequence, there is a trade-off between the maximum delay and bandwidth for a certain bandwidth ripple. The filter response result from the sum of each single stage response shows a maximum delay of $\tau_{\max} = 0.16$ ns for bandwidth of $\Delta f_{\mathrm{BW}} = 8.6$ GHz and a ripple ($\Delta\tau$) of 5 ps.

The plot of the normalized group delay at resonance for the two stage lattice RRAPF in Fig. 2**a** is shown in Fig. 8. After decreasing κ_2, while κ_1 is fixed at 0.9,

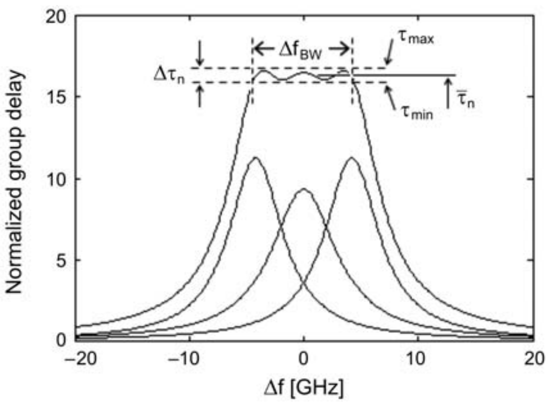

Fig. 7. Normalized group delay response of three stage cascaded RRAPF with lossless as in Fig. 1**b**, where the coupling coefficients and phase shifters of each single stage have been adjusted to yield a broadband group delay.

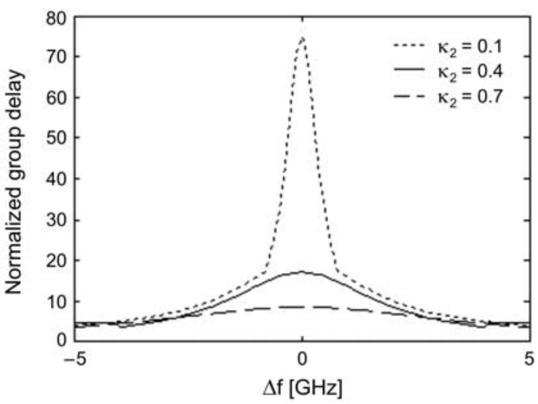

Fig. 8. Normalized group delay response of two stage lattice RRAPF with lossless as in Fig. 2**a**, for various coupling coefficients of $\kappa_2 = 0.1$, 0.4 and 0.7, while $\kappa_1 = 0.9$.

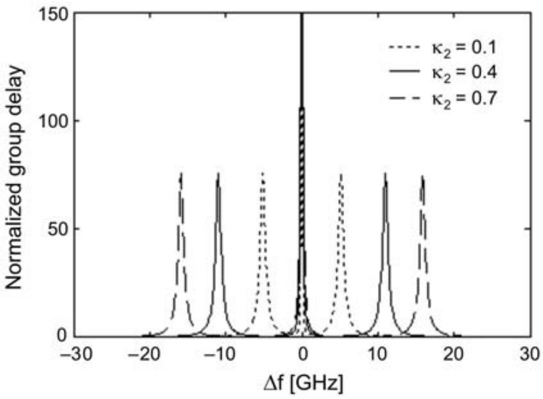

Fig. 9. Normalized group delay response of two stage lattice RRAPF with lossless as in Fig. 2**a**, for various coupling coefficients of κ_2 = 0.1, 0.4 and 0.7, while κ_1 = 0.1.

becomes a larger positive value and sharper compared with those with the result in Fig. 3 at the resonant point. The use of such configuration as a dispersion compensation filter is limited by unwanted additional sidemode peaks around the resonant point as shown in Fig. 9. A possible solution for realizing only a single group delay peak is obtained for the coupling coefficient κ_1, higher than 0.5.

5. Conclusions

Multi-stage ring resonator all-pass filters can be used as dispersion compensation. As shown above, the bandwidth utilization can be increased by increasing the number of filter stages. By appropriately adjusting the coupling coefficient κ_i and the phase shift φ_i of each single stage for cascaded RRAPF, a broadband group delay response can be achieved. Using lattice RRAPF, a normalized group delay at resonance with larger positive value and sharper is achieved compared with those of the cascaded RRAPF. For lattice RRAPF, a possible solution for realizing only a single group delay peak is obtained for coupling coefficient κ_1, higher than 0.5.

References

[1] VAN DE STADT H., *Ring interferometers with unit transmittance*, Applied Optics **24**(15), 1985, pp. 2290–2292.

[2] MADSEN C.K., LENZ G., BRUCE A.J., CAPUZZO M.A., GOMEZ L.T., NIELSEN T.N., BRENER I., *Multistage dispersion compensator using ring resonators*, Optics Letters **24**(22), 1999, pp. 1555–1557.

[3] MADSEN C.K., LENZ G., BRUCE A.J., CAPUZZO M.A., GOMEZ L.T., SCOTTI R.E., *Integrated all-pass filters for tunable dispersion and dispersion slope compensation*, IEEE Photonics Technology Letters **11**(12), 1999, pp. 1623–1625.

[4] LENZ G., MADSEN C.K., *General optical all-pass filter structures for dispersion control in WDM systems*, Journal of Lightwave Technology **17**(7), 1999, pp. 1248–1254.

[5] MADSEN C.K., *Optical all-pass filters for polarization mode dispersion compensation*, Optics Letters **25**(12), 2000, pp. 878–880.

[6] MADSEN C.K., ZHAO J.H., *Optical Filter Design and Analysis: A Signal Processing Approach*, Wiley, New York, 1999.

[7] SCHWELB O., *Generalized analysis for a class of linear interferometric networks. I. Analysis*, IEEE Transactions on Microwave Theory and Techniques **46**(10), 1998, pp. 1399–1408.

[8] YUPAPIN P.P., SAEUNG P., LI C., *Characteristics of complementary ring-resonator add/drop filters modeling by using graphical approach*, Optics Communications **272**(1), 2007, pp. 81–86.

Received March 3, 2008
in revised form August 7, 2008